

04,08,09

Radiation-Stimulated Transformations $\text{Yb}^{3+} \rightarrow \text{Yb}^{2+}$ and $\text{Yb}^{3+} \rightarrow \text{Yb}^{3+}$ in Single Crystals and Nanoceramics $\text{CaF}_2:\text{YbF}_3$

© M.Kh. Ashurov¹, I. Nuritdinov², S.T. Boyboboeva^{2,3,¶}

¹Fonon Research and Production Association,
Tashkent, 700054 Uzbekistan

²Institute of Nuclear Physics of the Academy of Sciences of the Republic of Uzbekistan,
Tashkent, 1000214 Uzbekistan

³Tashkent Regional Chirchik State Pedagogical Institute,
111700 Uzbekistan

¶ E-mail: sohibaboyboboeva@gmail.com

Received May 13, 2022

Revised May 13, 2022

Accepted May 23, 2022

The radiation resistance of $\text{CaF}_2:\text{YbF}_3$ (3 mol.% YbF_3) laser ceramics and a single crystal of similar composition (3.6 mol.% YbF_3) exposed to gamma rays in a ^{60}Co source is studied. The non-irradiated samples have been shown to be similar in spectral characteristics. After the $\text{CaF}_2:\text{YbF}_3$ crystals and ceramics γ -irradiation and the following time exposure, along with transformations $\text{Yb}^{3+} \rightarrow \text{Yb}^{2+}$, configurational $\text{Yb}^{3+} \rightarrow \text{Yb}^{3+}$ transitions between different states of Yb^{3+} ions in the structure of samples are carried out, with the participation of interstitial F_i ions.

Keywords: radiation resistance, laser ceramics, gamma rays, spectral characteristics defects.

DOI: 10.21883/PSS.2022.10.54233.379

1. Introduction

Recently, research efforts have been directed towards studying the properties of Yb^{3+} -doped CaF_2 single crystals and nanoceramics as promising laser materials pumped by laser diodes with the possibility of obtaining tunable laser radiation [1–9]. Among many kinds of host materials, CaF_2 is one of the first materials to be intensively examined for possible lasing [9], which has also been used to study the optical properties of both Yb^{3+} and Yb^{2+} ions. The Yb^{3+} ion is interesting because of its strong IR luminescence that can be easily pumped with conventional 940 and 980 nm laser diodes [10,11]. Yb^{2+} doped into CaF_2 is interesting because of its intense and broad yellow-green luminescence [12,13]. It is known that ytterbium ions can simultaneously enter the structure of crystals and nanoceramics in both Yb^{2+} and Yb^{3+} states, in various symmetric environments. The absorption characteristics of Yb^{3+} ions in CaF_2 crystals have been investigated in more detail than those of Yb^{2+} ions. It is known that Yb^{2+} ions enter the place of Ca^{2+} in the crystal lattice, which occupies cubic O_h positions in the lattice. When Yb enters the Yb^{3+} state, in order to maintain the electro neutrality of the system, it is necessary to compensate for an additional positive charge, which, as a rule, is carried out by negatively charged interstitial fluorine ions F_i^- . If crystals are synthesized under reducing conditions with an excess of fluorine at a relatively low (< 0.5 at.%) content of Yb ions, then, along with cubic (O_h) centers without local charge compensation, Yb^{3+} centers with tetragonal symmetry (C_{4v}), in which the F_i^- ion occupies a nearest-neighbor

(NN), as well as trigonal symmetry (C_{3v}), where the F_i^- ions are in the positions of the interstitial position next to the NN (NNN) [11,14–16]. At relatively high Yb contents, activator ions form various cluster states [8,17–20]. Such a complex structure of impurity centers leads to the formation of absorption spectra with broad bands. Depending on the growth conditions, the presence of co-dopant and the effect of ionizing radiation, the ratio of Yb centers can change, which is important in controlling the performance of these materials [8,12,13,17–20].

One priority issue in quantum electronics is the development of high-power lasers. In this context, fluorides offer important advantages, because the non-linear optical effects responsible for losses at high beam powers are substantially weaker in this class of materials. Among Yb-doped fluoride hosts, the $\text{CaF}_2:\text{Yb}^{3+}$ system offers the most attractive combination of physicochemical properties and technological aspects.

One serious innovation in optical materials research is laser ceramics [18,21–29]. Recently, attempts have been made to improve the kinetic and other characteristics of the laser and scintillation properties of fluoride materials by creating optical fluoride ceramics. The transition to ceramics improves the thermo-physical and mechanical characteristics (thermal conductivity, micro-hardness, and fracture toughness) of materials. The attractiveness of ceramics is determined by its properties such as the ability to create large-sized ceramic samples, high thermal conductivity, and a high threshold of thermal destruction. In this regard, the use of ceramics as an active medium

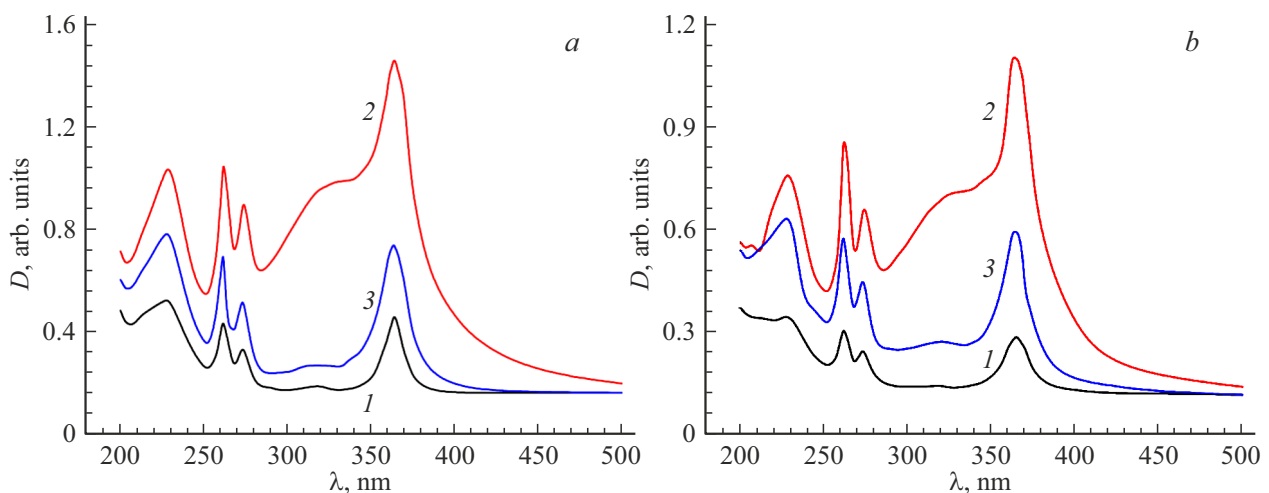


Figure 1. Optical absorption spectra of the *a*) $\text{CaF}_2:\text{YbF}_3$ crystal (3.63 mol.%) and *b*) nanoceramic $\text{CaF}_2:\text{YbF}_3$ (3 mol.%), in the UV-region: initial (curves 1), γ -irradiated with a dose of 10^5 rad (curves 2), and kept for 1 day after γ -irradiation (curves 3).

for high-power lasers and scintillators with the necessary resolution is very promising. In addition, the technology of manufacturing ceramics is more economical in comparison with the production of single crystals by traditional growth methods.

However, the radiation characteristics of fluoride nanoceramics, stimulated by exposure to radiation, are not fully understood and detailed studies in this direction are required. This kind of research is very promising from the point of view of expanding the use of nanoceramic materials in laser, scintillation, and other fields of science and technology.

The purpose of this work was the investigation of radiation-stimulated changes in various Yb centers in $\text{CaF}_2:\text{YbF}_3$ (3 mol.% YbF_3) laser ceramics in comparison with a single crystal of similar composition (3.6 mol.% YbF_3).

2. Experimental

Crystals were grown by vertical directional solidification [30,31]. As a fluorination agent („cleaner“), lead fluoride was used. Ceramics were produced by hot molding [21,22]. In measurements, we used samples cut from the $\text{CaF}_2:\text{YbF}_3$ single crystals and ceramics (hereafter, simply „crystals“ and „ceramics“) in the form of parallelepipeds $1 \times 5 \times 10$ mm in dimensions and polished to optical quality.

Optical absorption spectra were measured on Lambda 35 (190–1100 nm) and Specord M-40 (200–800 nm) spectrophotometers. The samples were exposed to gamma rays in a ^{60}Co source to gamma doses from 10^5 to 10^8 rad. No corrections were made to the measured spectra.

3. Results and discussion

The optical absorption spectra of the initial crystalline and ceramic samples had identical optical absorption spectra,

which contained bands in the UV-region with maxima at 214, 227, 260, 271, 320, and 360 nm (Fig. 1, *a* and *b*, curves 1), as well as a group of lines in the wavelength range of 860–1060 nm, with maxima at 922, 940, 944, 964, 978, 1010, and 1030 nm in the IR region (Fig. 2, *a* and *b*, curves 1). The intensities of the observed absorption bands in a range of 214–360 nm for crystalline and ceramic samples correspond to electronic transitions from the 1S_0 ($4f^{14}$) to the $4f^{14}5d$ levels of the Yb^{2+} ions, and in the range of 920–1060 nm — to the $^2F_{7/2}$ – $^2F_{5/2}$ transitions of the Yb^{3+} ions [20,31]. Since f – d transitions are allowed, in contrast to f – f transitions, the intensities of the corresponding absorption bands differ by about a factor of 10^4 [32].

Under excitation by gamma irradiation at room temperature in the doses range of 10^5 – 10^8 rad, the intensities of all bands of Yb^{2+} ions in the wavelength range of 200–400 nm increase (Figs. 1 and 2, curves 2), the intensities of the line groups of Yb^{3+} ions in the range of 860–1060 nm decrease slightly in both types of samples, which indicates a valence $\text{Yb}^{3+} \rightarrow \text{Yb}^{2+}$ transition on impurity ions [11,12,14,19,20].

Analysis and comparison of the optical absorption spectra of the initial and irradiated samples, and samples kept after irradiation at room temperature show that in the samples under γ -irradiation and held after irradiation, in addition to $\text{Yb}^{3+} \rightarrow \text{Yb}^{2+}$ transitions, complex $\text{Yb}^{3+} \rightarrow \text{Yb}^{3+}$ transformations occur within the Yb^{3+} states themselves.

Under γ -irradiation of the samples, the intensity absorption band of the 979 nm strongly decreases, the intensities of the bands with maxima at 945, 966, and 990 nm decrease slightly, and intensities of the bands with maxima at 920 and 962 nm increase (Fig. 3, *a* and *b*, curves 1). After the termination of irradiation, the spectrum is restored, but after a day it is not completely restored to the state of the spectrum in non-irradiated samples (Fig. 3, *a* and *b*, curves 2 and 3). One day after irradiation, the number of centers responsible for absorption bands with maxima

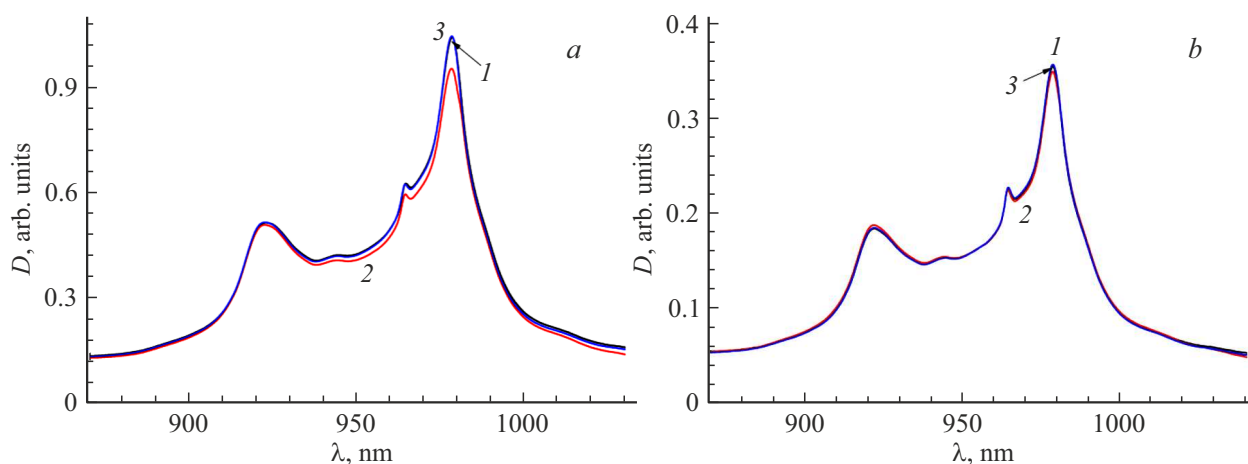


Figure 2. Optical absorption spectra of the *a*) $\text{CaF}_2:\text{YbF}_3$ crystal (3.63 mol.%) and *b*) nanoceramics $\text{CaF}_2:\text{YbF}_3$ (3 mol.%), in the IR-region: initial (curves 1), γ -irradiated with a dose of 10^5 rad (curves 2), and kept for 1 day after γ -irradiation (curves 3).

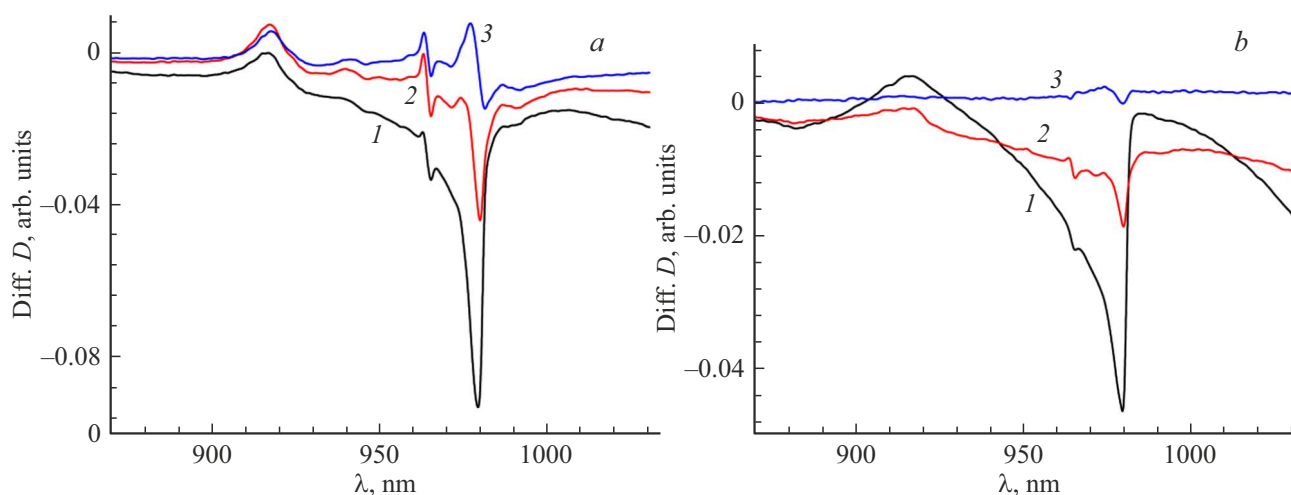


Figure 3. Difference absorption spectra for *a*) crystal $\text{CaF}_2:\text{YbF}_3$ (3.63 mol.%) and *b*) nanoceramic $\text{CaF}_2:\text{YbF}_3$ (3 mol.%): γ -irradiated with a dose of 10^5 rad and initial sample (curves 1); kept after irradiation for 1 hour and initial (curves 2); kept for 1 day after γ -irradiation and initial sample (curves 3).

in the UV-region at 262, 274, 320, and 365 nm in the irradiated samples is somewhat larger than in the initial non-irradiated state, but the concentration of centers associated with bands in the IR-region at 944, 965, 980 nm is less (Fig. 3, *a* and *b*, curves 3). This indicates that, during the irradiation of single crystals and nanoceramics based on $\text{CaF}_2:\text{YbF}_3$, especially after holding them at room temperature, not only transformations of the $\text{Yb}^{3+} \rightarrow \text{Yb}^{2+}$ type, but also transitions of the $\text{Yb}^{3+} \rightarrow \text{Yb}^{3+}$ type occur, which are surrounded by different symmetries.

According to the data of works [8,11,15,16,20], the absorption observed in $\text{CaF}_2:\text{YbF}_3$ samples in a range of 900–1000 nm is due to the following: bands with maxima at 921 and 963 nm are associated with cubic O_h symmetry; 966 nm, with tetragonal C_{4v} symmetry; 910, 936 nm, with trigonal C_{3v} symmetry; at 944 and 956 nm, small clusters are composed; at 980 nm, hexametric clusters

occur. Our experiments have shown that the 921, 965, and 981 nm bands are complex, and they overlap the absorption of several Yb^{3+} centers. This is also evidenced by studies of the temperature dependence of the absorption of $\text{CaF}_2:\text{YbF}_3$ crystals in [20].

Interestingly, while the bands intensities decrease with increasing temperature in non-irradiated samples (921, 940, 962, and 976 nm), in irradiated samples intensities increase over their storage time after irradiation. The concentration of such centers in the irradiated samples becomes somewhat higher one day after ceasing the irradiation. The difference spectra of the γ -irradiated and initial samples exactly coincide with the low-temperature absorption spectrum of the non-irradiated sample shown in Fig. 8 in [20]. This effect can be explained as follows. During irradiation of samples with γ -rays, interstitial fluorine ions, having received the energy of electronic excitations, move away from tetragonal

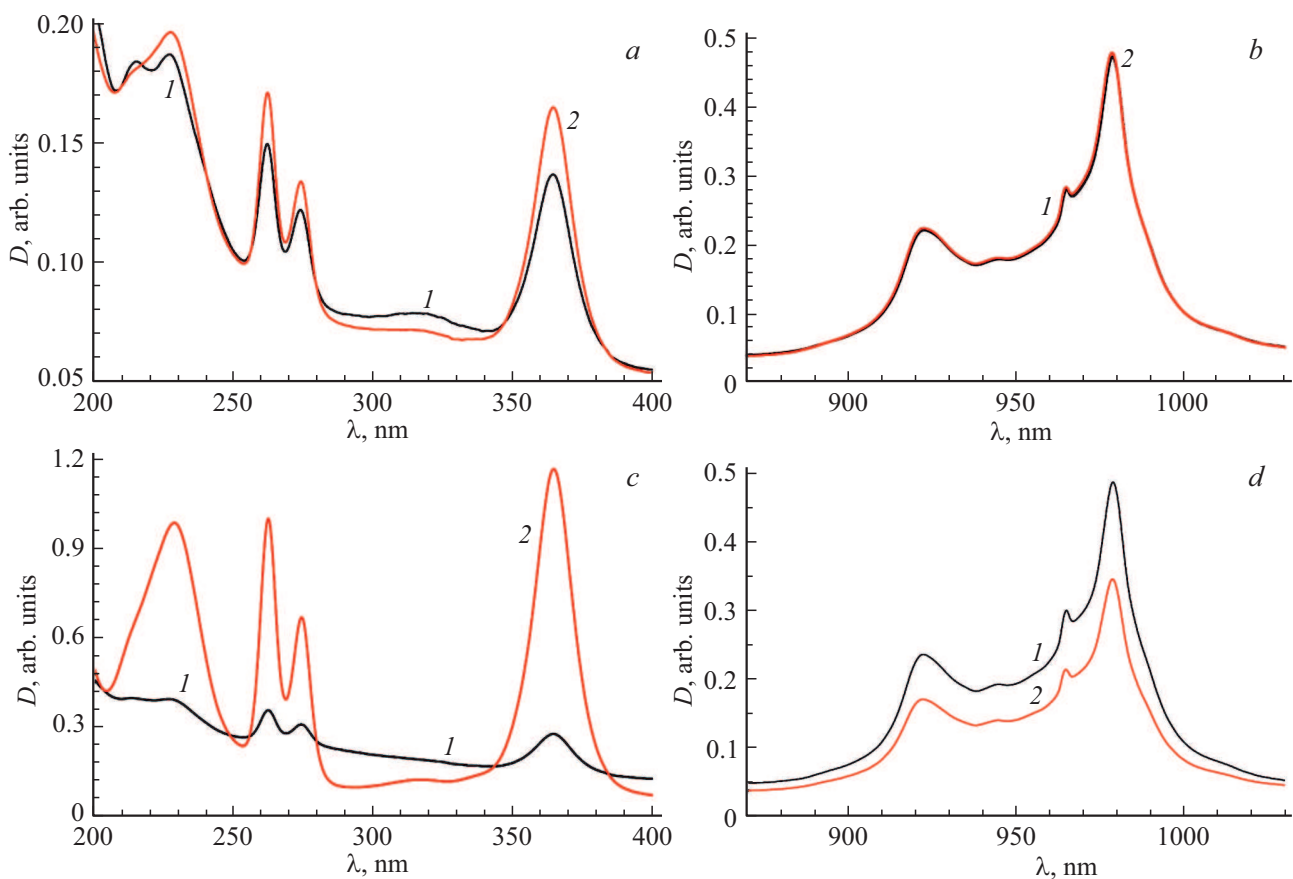


Figure 4. Optical absorption spectra of $\text{CaF}_2:\text{YbF}_3$ crystal (3 mol.%) and ceramics (3 mol.%) in the UV-region of the spectrum (*a* — crystal, *c* — ceramics) and IR-region (*b* — crystal, *d* — ceramics): initial (curves 1) and after annealing at a temperature of 600°C (curves 2).

and trigonal centers, as well as from small and hexameric clusters. In this case, along with a decrease in these centers (as evidenced by a decrease in the intensities of the 940, 944, 965, and 981 nm bands after irradiation, see Fig. 3), the number of cubic centers increases (there is a slight increase in the intensities of the 921, 964, and 976 nm bands after irradiation, see Fig. 3). At this cubic Yb^{3+} O_h symmetry, electrons can be captured, transforming into Yb^{2+} type. Over time, the Yb^{2+} states can be thermally ionized, while the cubic Yb^{3+} centers increase, which over time stimulates an increase in the intensities of their absorption bands at 921, 963, and 976 nm.

Comparison of the difference spectra of irradiated and stored after irradiation single-crystal and nanoceramic samples (Fig. 3) shows that, on the one hand, there are general tendencies; on the other hand, the distinctive features of the processes occur in single-crystal and nanoceramic samples during irradiation and their holding. The main differences are: a significantly small amount of Yb^{3+} ions passing into the Yb^{2+} state in nanoceramics as compared to single crystals; fast, in comparison with single crystals, reduction of Yb^{3+} centers irradiated nanoceramic samples to the initial state; as well as a change in the ratio of different Yb^{3+} centers in γ -irradiated samples. We assume that these

differences are due to the presence of a large number of interface grain boundaries and boundaries between nanolayers of nanoceramic samples.

The absorption spectrum of crystal and ceramic samples was measured after irradiation with a dose of 10^8 rad, exposure for 6 months in the dark, followed by annealing at a temperature of 600°C . Comparative measurements of the absorption spectrum nanoceramic samples show that the intensity of the absorption spectrum after annealing does not return to its initial state. In crystals, the intensity of the absorption band returns almost to its initial state (Fig. 4).

From this, it can be assumed that during the irradiation of single crystals and nanoceramics based on $\text{CaF}_2:\text{YbF}_3$, the valence transformation of Yb ions $\text{Yb}^{3+} \rightarrow \text{Yb}^{2+}$ and configurational $\text{Yb}^{3+} \rightarrow \text{Yb}^{3+}$ transitions between different states of Yb^{3+} ions in the structure of samples are carried out, with the participation of interstitial F_i ions. During holding and after annealing, quasi-stable fluorine ions F_i that have left their places return to their initial state. This is due to the fact that in crystals, due to the absence of boundaries that impede the movement of fluorine ions, they return to their initial state. However, some damage to the crystal structure remains in the crystals, where interstitial fluorine ions are retained.

In ceramics, such areas can be interfaces between „grains“ and „voids“. After annealing the ceramics at a temperature of 600°C, intensity of the absorption band does not return to its initial state, which indicates that the orientation of crystallite changes structure in the ceramic during annealing; as a result, voids may change where interstitial fluorine ions are retained.

4. Conclusions

The as-prepared crystalline and ceramic $\text{CaF}_2:\text{YbF}_3$ samples have identical optical absorption spectra which contain absorption bands corresponding of divalent ytterbium in the spectral range of 200–360 nm and bands corresponding to trivalent ytterbium in the range of 922–980 nm. Irradiation of the crystalline and ceramic samples to gamma doses from 10^5 to 10^8 rad increases the Yb^{2+} concentration and slightly decreases Yb^{3+} concentration, which a valence $\text{Yb}^{3+} \rightarrow \text{Yb}^{2+}$ transition on impurity ions indicates. After the $\text{CaF}_2:\text{YbF}_3$ crystals and ceramics γ -irradiation and the following time exposure, along with transformations $\text{Yb}^{3+} \rightarrow \text{Yb}^{2+}$, configurational $\text{Yb}^{3+} \rightarrow \text{Yb}^{3+}$ transitions between different states of Yb^{3+} ions in the structure of samples are carried out, with the participation of interstitial F_i ions. After annealing at a temperature of 600°C, the intensity of absorption bands in crystals returns almost to its initial state, while in ceramics they do not return. All this suggests that there are not only structural defects common to both ceramic samples and crystals but also defects present only in ceramics. This seems to be associated with structural imperfections related to grain boundaries, as well as to twin boundaries present in ceramics [26].

Conflicts of interest

The authors declare that they have no conflict of interest.

References

- [1] L.D. Deloach, S.A. Payne, L.L. Chase, L.K. Smith, W.F. Krupke. *IEEE J. Quantum Electron.* **29**, 179 (1993).
- [2] Yu.K. Voronko, V.V. Osiko, I.A. Shcherbakov. *Zh. Eksp. Teor. Fiz.* **56**, 1, 151 (1969).
- [3] A. Lucca, G. Debourg, M. Jacquemet, F. Druon, F. Balembois, P. Georges, P. Camy, J.L. Doualan, R. Moncorgé. *Opt. Lett.* **29**, 23, 2767 (2004).
- [4] A. Jouini, A. Brenier, Y. Guyot, G. Boulon, H. Sato, A. Yoshikawa, K. Fukuda, T. Fukuda. *Cryst. Growth Design* **8**, 3, 808 (2008).
- [5] M. Siebold, S. Bock, U. Schramm, B. Xu, J.L. Doualan, P. Camy, R. Moncorgé. *Appl. Phys. B* **97**, 2, 327 (2009).
- [6] G. Machinet, J. Lhermite, D. Descamps, G. Andriukaitis, D. Adams, A. Pugžlys, A. Baltuška, E. Cormier. *Appl. Phys. B* **111**, 3, 495 (2013).
- [7] P.A. Popov, P.P. Fedorov, S.V. Kuznetsov, V.A. Konyushkin, V.V. Osiko, T.T. Basiev. *Dokl. Phys.* **53**, 4, 198 (2008).
- [8] I. Nicoara, L. Lighezan, M. Enculescu, I. Enculescu. *J. Crystal Growth* **310**, 7–9, 2026 (2008).
- [9] W.F. Krupke. *IEEE J. Quantum Electron.* **6**, 6, 1287 (2000).
- [10] Yu.K. Voronko, V.V. Osiko, I.A. Shcherbakov. *Zh. Eksp. Teor. Fiz.* **56**, 1, 151 (1969).
- [11] M. Ito, C. Goutaudier, Y. Guyot, K. Lebbou, T. Fukuda, G. Boulon. *J. Phys: Condens. Matter* **16**, 8, 1501 (2004).
- [12] A.A. Kaplyanskii, V.N. Medvedev, P.L. Smolyanskii. *Opt. Spectrosc.* **41**, 615 (1976).
- [13] E.G. Reut. *Opt. Spektrosc.* **40**, 1, 99 (1976).
- [14] J. Kirton, S.D. McLaughlan. *Phys. Rev.* **155**, 2, 279 (1967).
- [15] E. Loh. *Phys. Rev.* **184**, 2, 348 (1969).
- [16] J. Corish, P.W.M. Jacobs, C.R.A. Catlow, S.H. Ong. *Phys. Rev. B* **25**, 10, 6425 (1982).
- [17] S. Lizzo, A.J. Meijerink, G. Dirksen, G. Blasse. *J. Lumin.* **63**, 5, 223 (1995).
- [18] M.Kh. Ashurov, S.T. Boibobeva, I. Nuritdinov, E.A. Garibin, A.A. Demidenko, S.V. Kuznetsov, P.P. Fedorov. *Inorg. Mater.* **52**, 8, 842 (2016).
- [19] I. Nicoara, M. Stef, A. Pruna. *J. Crystal Growth* **310**, 7, 1470 (2008).
- [20] S.M. Kaczmarek, T. Tsuboi, M. Ito, G. Boulon, G. Leniec. *J. Phys.: Cond. Matter* **17**, 25, 3771 (2005).
- [21] P.P. Fedorov. In: B. Denker, E. Shklovsky (Eds). *Handbook on Solid-State Lasers: Materials, Systems and Applications*. Woodhead Pub. Ltd, UK (2013). P. 82–109.
- [22] M.Sh. Akchurin, T.T. Basiev, A.A. Demidenko, M.E. Doroshenko, P.P. Fedorov, E.A. Garibin, P.E. Gusev, S.V. Kuznetsov, M.A. Krutov, I.A. Mironov, V.V. Osiko, P.A. Popov. *Opt. Mater.* **35**, 3, 444 (2013).
- [23] T.T. Basiev, M.E. Doroshenko, P.P. Fedorov, V.A. Konyushkin, S.V. Kuznetsov, V.V. Osiko, M.Sh. Akchurin. *Opt. Lett.* **33**, 5, 521 (2008).
- [24] P.A. Popov, K.V. Dukel'skii, I.A. Mironov, A.N. Smirnov, P.A. Smolyanskii, P.P. Fedorov, V.V. Osiko, T.T. Basiev. *Dokl. Phys.* **52**, 1, 7 (2007).
- [25] M.E. Doroshenko, A.A. Demidenko, P.P. Fedorov, E.A. Garibin, P.E. Gusev, H. Jelinkova, V.A. Konyushkin, M.A. Krutov, S.V. Kuznetsov, V.V. Osiko, P.A. Popov, J. Shulc. *Phys. Status Solidi C* **10**, 6, 952 (2013).
- [26] M.Sh. Akchurin, R.V. Gainutdinov, E.A. Garibin, Yu.I. Golovin, A.A. Demidenko, K.V. Dukel'skii, S.V. Kuznetsov, I.A. Mironov, V.V. Osiko, A.N. Smirnov, N.Yu. Tabachkova, A.I. Tyurin, P.P. Fedorov, V.V. Shindyapin. *Perspekt. Mater.* **5**, 1, 5 (2010).
- [27] Z. Liu, B. Mei, J. Song, D. Yuan, Z. Wang. *J. Alloys Compd.* **646**, 760 (2015).
- [28] A. Lyberis, A.J. Stevenson, A. Sukanuma, S. Ricaud, F. Druon, F. Herbst, D. Vivien, P. Gredin, M. Mortier. *Opt. Mater.* **34**, 6, 965 (2012).
- [29] P. Aballea, A. Sukanuma, F. Druon, J. Hostalrich, P. Georges, P. Gredin, M. Mortier. *Optica* **2**, 4, 288 (2015).
- [30] P.P. Fedorov, V.V. Osiko. In: *Optical and Optoelectronic Materials / Ed. P. Capper*. Wiley, N.Y. (2005). P. 339–356.
- [31] A.E. Angervaks, A.S. Shcheulin, A.I. Ryskin, E.A. Garibin, M.A. Krutov, P.E. Gusev, A.A. Demidenko, S.V. Kuznetsov, E.V. Chernova, P.P. Fedorov. *Inorg. Mater.* **50**, 7, 733 (2014).
- [32] A.S. Shcheulin, A.E. Angervaks, T.S. Semenova, L.F. Koryakina, M.A. Petrova, P.P. Fedorov, V.M. Reiterov, E.A. Garibin, A.I. Ryskin. *Appl. Phys. B* **111**, 4, 551 (2013).